Civil Engineering Infrastructures Journal, 50(2): 311 – 332, December 2017
Print ISSN: 2322-2093; Online ISSN: 2423-6691
DOI: 10.7508/ceij.2017.02.007

Corner Crack Effect on the Seismic Behavior of Steel Plate Shear Wall System

Broujerdian, V.[1*], Shayanfar, M.A.[2] and Ghamari, A.[3]

[1] Assistant Professor, Department of Civil Engineering, Faculty, Iran University of Science and Technology, Tehran, Iran.
[2] Associate Professor, Department of Civil Engineering, Faculty, Iran University of Science and Technology, Tehran, Iran.
[3] Ph.D. Candidate, Department of Civil Engineering, Faculty, Iran University of Science and Technology, Tehran, Iran.

Received: 24 Dec. 2016; Revised: 18 Jul. 2017; Accepted: 25 Jul. 2017

ABSTRACT: Although, experimental studies have reported fracture at the corner of Steel Plate Shear Walls (SPSW), no study has been performed to investigate the crack effect, yet. Therefore, in this paper, the effect of crack at the corner of SPSWs on the seismic behavior of the system was investigated. Two probable cracks, that have been studies at the corner of SPSWs utilizing extended Finite Element method based on cohesive crack approach, are initial horizontal crack and initial vertical crack. Numerical results indicated that small initial crack does not have considerable effect on the seismic behavior of SPSW. In addition, the horizontal crack is more effective than vertical crack. Since SPSWs with long initial horizontal crack are ruptured suddenly, so they could not be utilized as a lateral resisting in seismic zone. Nevertheless, no ruptures occur in SPSWs with vertical cracks. Therefore, SPSWs with horizontal crack must be repaired, but no repairing is needed in SPSWs with initial vertical cracks.

Keywords: Crack, Extended Finite Element Method, Response Modification Factor, Seismic Behavior, Steel Shear Wall.

INTRODUCTION

Steel Plate Shear Wall (SPSW) is a lateral load bearing system which has shown a good behavior in past earthquakes, and its performance is corroborated by numerical and experimental studies (Hatami et al., 2012; Abdollahzadeh et al., 2017). In addition to its ductile behavior, considerable stiffness and strength of steel shear wall has made it technically and economically suitable to be used as a load bearing system in different structures all over the world (Driver et al., 1998; Abdollahzadeh and Malekzadeh, 2013). However, a constructional problem could weaken this system and change its behavior to a brittle one.

The main function of SPSW is to resist horizontal story shear and overturning moment engendered by lateral loads (Astane-Asl, 2001). In general, SPSW system is consisted of a steel plate wall (infill steel plate), two boundary columns (VBE) and horizontal floor beams (HBE) shown in

* Corresponding author E-mail: broujerdian@iust.ac.ir

Figure 1. The infill steel plate connects to the VBEs and HBEs surrounding it by a Fishplate as shown in Figure 1. In other words, Fishplates are used along boundary frame members to connect infill plate to the beams and columns. The Bolted or Fillet weld can be utilized to contact the infill plate to the Fishplate, but only weld can be utilized to contact the Fishplate to the boundary elements, HBE and VBE. Since Fishplate and infill plate have low thickness, the welding between the Fishplate and boundary elements is susceptible to crack. In other words, crack between the Fishplate and boundary element is undeniable. The main flaw is that repairing the recognized crack is very difficult, because removing the injured weld and welding the thin plate again cannot result to a good quality of fabrication. Therefore, investigated in this study, it is important to know what kind of crack is crucial between Fishplate and boundary elements.

The quality of real fabrication on the civil projects is much lower than experimental test fabrication. However, experimental studies are carefully performed with high quality of fabrication, to prevent fracture, fracture of welding or crack propagation in welds have occurred in several testing (Guendel et al., 2011; Dubina and Dinu, 2014; Shekastehband et al., 2017). Therefore, it is expected that crack propagation on real SPSWs under real seismic loading be evaluated more. Though, by taking care of fabrication, some of experiments have failed due to crack propagation in the weld or infill plate, cracked SPSW have not yet been comprehensively investigated. Although a great deal of research is devoted to crack analysis of steel plates, none of them simulates the steel shear wall boundary conditions.

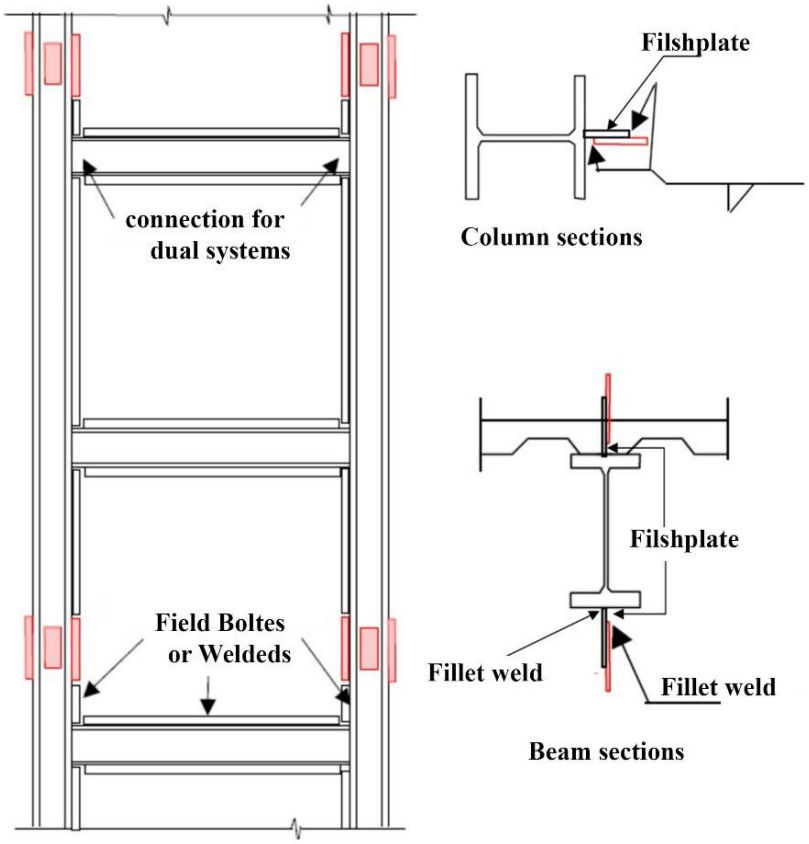

Fig. 1. Shop-welded, field-bolted steel plate shear walls (Astane-Asl, 2001)

Till now, cracked SPSW has been studied by authors for crack propagation at mid height (corner and central crack) of infill steel plate when two separate plates are utilized as infill steel plate (Broujerdian et al., 2016). Results showed that seismic behavior of shear wall would be affected by the crack growth. Also, more studies are required to investigate complete effects of the cracks on the behavior of SPSWs.

Considering a steel plate under pure shear, where the shear loading reaches a certain value, the plate buckles under the induced diagonal compressive stresses, and it shows an out-of-plane deformation. In the steel shear wall system, plate buckling is usually the dominant mode of failure. Therefore, the influence of cracks on the buckling and load bearing capacity of thin-walled panels must be investigated and considered in the design process.

Sih and lee (1968) investigated the behavior of cracked plate under tensile and compressive axial loads. They showed that as crack length increases, pre-buckling capacity of plate reduces. Shaw and Huang (1990) studied the buckling behavior of cracked plate under tensile force using Finite Element method (Shaw and Huang, 1990). In that study, the effect of crack length, boundary conditions and biaxial loading were investigated. Riks et al. (1992) investigated buckling and post-buckling behavior of cracked plate under tensile load using Finite Element method. According to their results, changing the post-buckling shape would result in stress accumulation at the tip of crack. This accumulation is intensified as the crack length increases. In line with that research, several studies have been conducted into the effect of cracks on thin panels under pure shear (Dubina, and Dinu, 2014), axial compression (Bert and Devarakonda, 2003) and axial tension (Brighenti, 2005).

As pointed before, previous studies mainly focus on the behavior of individual plates out of the structure. Therefore, the effects of crack in the connection of shear plate to boundary element (beam and column) on the behavior of a complete steel shear wall system and its seismic design parameters have not been considered yet. In this study, the effect of cracks in steel shear walls on the overall behavior of structures is considered. For this purpose, the Extended Finite Element Method (XFEM) is used. Belytschko et al. (2003) originally proposed this method. XFEM has become increasingly popular to solve different fracture problems (Xie et al., 2016; Nasirmanesh, and Mohammadi, 2017; Campilho et al., 2011; Golewski et al., 2012; Wang et al., 2012).

METHOD OF STUDY

In this paper, the effect of cracks at the corner of shear walls as the probable cracks is investigated numerically. All studies are performed numerically using XFEM. Since the base material is steel, which is a ductile material, the crack is modeled as a cohesive one based on Dugdale model (Belytschko et al., 2003). Due to the geometric nonlinearity of SPSW arising from its low thickness, compatibility and equilibrium equations are formulated based on large deformation assumption. To simulate the material nonlinearity, the elastic-plastic behavior with yield surface of von Mises yield criterion is used. ANSYS software (ANSYS, 2016) is used in combination with ABAQUS (Hibbitt et al., 2012) to accelerate the modeling and analysis process. The path of crack growth is detected in ABAQUS using Solid elements, and then all elements are simulated in the form of Shell in ANSYS by utilizing APDL capability. The main aim is to determine elastic and inelastic behavior of SPSW due to crack at the corner of the system. Therefore, the critical probable cracks, Figure 2, are recognized; horizontal or vertical cracks. In addition, the effect of initial crack length,

recognizing the critical cracks, the effect of length to height of SPSWs on the nonlinear behavior of the system, the effect of crack on the seismic parameters such as response modification factor, stiffness, ultimate strength, and energy absorption are evaluated.

Fundamentals of XFEM Method

Conventional FE methods have high computational costs owing to the extremely fine meshes needed in the regions around discontinuities such as notches and cracks. Several approaches that combine FE and analytical methods have been adopted in an attempt to overcome these problems. For instance, the remeshing technique, which updates an original mesh at each time step, is widely used for crack growth analyses, and the traction-separation law is frequently adopted to capture rapid changes in material properties instead of conventional stress-strain relationships (Hibbitt et al., 2012). However, the precedents in these approaches result in the loss of accuracy during the mapping of the stress distribution from the old mesh to new mesh, and are disadvantageous in modeling arbitrary crack growth.

To reduce the effort of remeshing on crack propagation, XFEM has been emerged that XFEM is an extension of classical Finite Element method using framework of partition of unity. The advantage of XFEM is that it removes the need to re-mesh in crack propagation problems. In the XFEM method, two additional displacement functions are added to the Finite Element solution space. Discontinuous function is one of these functions which dedicates displacement jump across the crack surface. The second function represents the singularity of crack tip. The displacement function can be presented as:

$$u = \sum_{i=1}^{N} N_i(x) \left[u_i + H(x) a_i + \sum_{a=1}^{4} F_a(x) b_i^a \right] \quad (1)$$

where $N_i(x)$: is the general nodal shape function, u_i: is the general nodal displacement vector associated with the continuous part of the Finite Element solution, *H(x)* : is the associated discontinuous jump function across the crack surfaces, a_i: is the product of the enriched degree of freedom vector, $F_a(x)$: is the associated elastic asymptotic crack-tip function, and b_i^a: is the product of the enriched freedom degree. The discontinuous jump function across the crack surfaces, *H(x)*, is given by:

$$H(x) = \begin{cases} 1 & if\ (x - x^*).n \geq 0 \\ -1 & otherwise \end{cases} \quad (2)$$

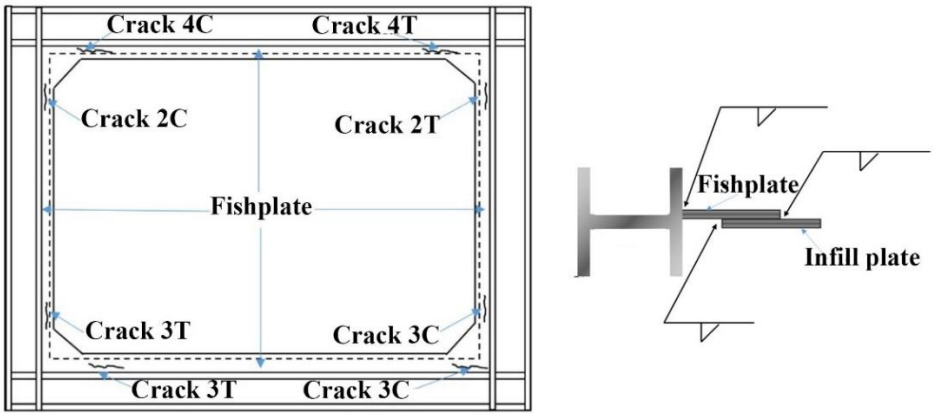

Fig. 2. Definition of crack

where, *x*: is a sample (Gauss) point, *x**: is the point on the crack closest to *x*, and *n*: is the unit outward normal to the crack at *x**. In an isotropic elastic material, $F_a(x)$ is given by:

$$F_a(x) = \begin{bmatrix} \sqrt{r}\sin\frac{\theta}{2}, \sqrt{r}\cos\frac{\theta}{2}, \\ \sqrt{r}\sin\theta\sin\frac{\theta}{2}, \sqrt{r}\sin\theta\cos\frac{\theta}{2} \end{bmatrix} \quad (3)$$

where (r, θ): is a polar coordinate system with its origin at the crack tip. $\theta = 0$ is tangent to the crack at the tip and $\sqrt{r}\sin\frac{\theta}{2}$ represents the discontinuity across the crack surfaces. Cohesive segment method is based on the cohesive elements with traction-separation behavior, which is given by:

$$t = \begin{Bmatrix} t_s \\ t_n \\ t_t \end{Bmatrix} = \begin{bmatrix} K_{ss} & 0 & 0 \\ 0 & K_{nn} & 0 \\ 0 & 0 & K_{tt} \end{bmatrix} \begin{Bmatrix} \delta_s \\ \delta_n \\ \delta_t \end{Bmatrix} = K\delta \quad (4)$$

where *t*, the nominal traction stress vector, consists of three components: t_s, t_n, and t_t with corresponding displacements of δ_s, δ_n, and δ_t (Hibbitt et al., 2012).

XFEM Method in ABAQUS Software

ABAQUS software (Hibbitt et al., 2012) allows implementing XFEM in both static and dynamic problems. In dynamic problems, only the use of implicit dynamic analysis procedure is possible. Two different methods are provided in ABAQUS in order to determine the initial position of crack. In the first method, user defines the initial crack. This is the method which is used in the present work to determine the initial crack position. In the second method, the software determines the initial crack during the analysis based on the maximum stress or principal strain criterion. After determining the initial crack, crack propagation occurs in a direction that the stress or principal strain is greater than the maximum damage value defined to the software. It is noteworthy that the user defines crack occurrence condition and crack growth condition as the damage initiation criteria and damage evolution law, respectively (Hibbitt et al., 2012). In this study, maximum principal stress damage, Maxps, is used as the crack initiation criterion, and energy-based damage evolution law based on a power law criterion is used as a measure of crack growth.

The Abaqus ductile fracture material model is based on phenomenological criterion for predicting the onset of damage due to nucleation, growth, and coalescence of voids. The criterion for fracture initiation is met when the following condition is satisfied:

$$\varpi_D = \int \frac{d\varepsilon^{pl}}{\varepsilon_D^{pl}(\eta)} = 1 \quad (5)$$

where the damage parameter ω_D: is a state variable increasing monotonically with plastic deformation. It is zero for undamaged material and equals one for totally damaged material. The model assumes that the equivalent plastic strain at the onset of fracture $\frac{d\varepsilon^{pi}}{\varepsilon_D^{pi}(\eta)}$ is a function of triaxiality η defined as Eq. (6).

$$\eta = -\frac{p}{q} \quad (6)$$

where *p*: is the hydrostatic stress, and q is the Mises equivalent stress. The equivalent plastic strain function $\frac{d\varepsilon^{pi}}{\varepsilon_D^{pi}(\eta)}$ was described by Johnson-Cook model (Johnson and Cook, 1983):

$$\varepsilon_D^{pl} = D_1 + D_2 e^{D_3\eta} \quad (7)$$

where coefficients D_1, D_2 and D_3 need to be determined. The integration of damage

parameter ω_D was evaluated numerically for all estimated sets of coefficients D_i.

Mesh Sensitivity and Buckling Analysis

The linear analysis option of the FE program was incorporated to predict the elastic shear buckling stress of perfect uncracked shear wall having a uniform mesh distribution. The Eigen-buckling method of this package and its ‘‘Shell’’ element were used as basic concepts. This four-node quadrilateral shell element is capable of modeling elastic behavior and can simulate both membrane and flexural behaviors. In addition, it has three rotational and three translational degrees of freedom per node.

Regarding the convergence study and verification of results, panels were divided into sufficient number of elements to allow for the development of shear buckling modes and displacements. The elastic buckling shear stress values derived from numerical analyses were compared to those obtained from Eq. (8).

$$\tau_{cr} = \frac{K_v \pi^2 E}{12(1 - \nu^2)} \tag{8}$$

$$K_v = \begin{Bmatrix} 5.34 + \dfrac{4}{(d/b)^2} & d/b \le 1 \\ 4 + \dfrac{5.34}{(d/b)^2} & d/b > 1 \end{Bmatrix} \tag{9}$$

where E, b and d : are the modulus of elasticity, length of plate and height of plate, respectively (Basler, 1961).

Figure 3 shows the variation of percentage errors obtained by comparing the Finite Element analysis results to the theoretical value for different number of incorporated elements. According to the results presented in Figure 3, the models with a mesh refinement of 30×30 (900 elements) produced results that were in good agreement with the theory and was therefore used as the minimum requirement.

The Finite Element modeling and analysis of cracked shear wall involve maximizing the precision associated with the calculation of stresses and displacements near cracks and the local effects imposed by the cracks on the overall response of panels. The first obvious solution to increase precision was to use denser Finite Element meshing near the cracks. Therefore, for meshing purposes, the panels were divided into three zones, namely the ‘‘crack tips’’ along the ‘‘crack sides’’ and ‘‘away’’ from the cracks.

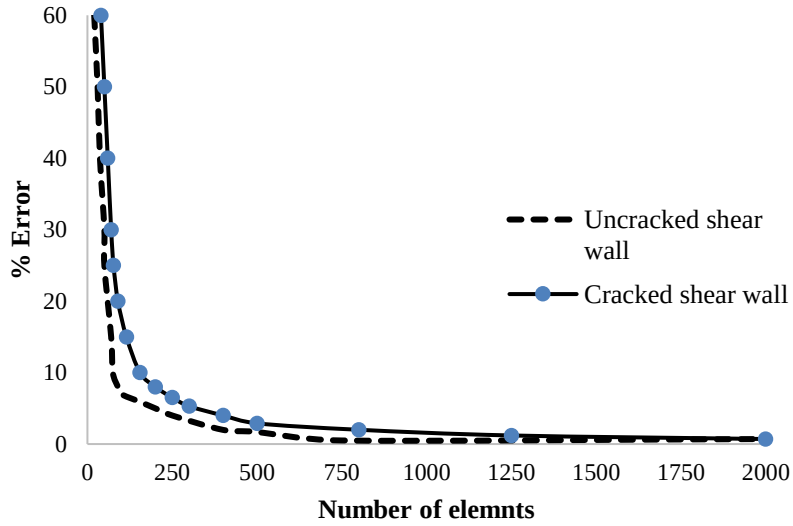

Fig. 3. Convergence studies and mesh sensitivity in uncracked

These divisions were suggested for assigning different mesh densities for zones relative to the position of cracks. According to a study conducted by Alinia and his colleagues (Alinia et al., 2007) due to stress concentration, very dense meshing is utilized near the crack tips. The element sizes were then gradually increased to the optimum size of uncracked panels as they parted away from cracks.

Verification of Numerical Modeling Process

For validating the numerical modeling process, the results of two experimental models, consisting of a SPSW without crack and a cracked steel plate, are compared to Finite Element modeling results. In the Finite Element model, shell element is used to all components of shear wall. The elements are meshed in a way that the nodes of the beam, columns and steel plate elements coincide. For a more tangled connection, nodes in one spot are merged. It must be noted that the probable constructional imperfection of steel shear wall is considered as a multiple of the first mode shape of buckling obtained by an elastic buckling analysis.

Numerical Modeling of Steel Full-Plate Shear Wall without Crack

The experimental report by Driver and co-workers (Driver et al., 1998), shown in Figure 4a, is considered as a benchmark to validate ANSYS Finite Element modeling of steel shear wall system without crack. The loading contains cyclic lateral forces off at each story level and two gravitational loads of "P" on top of the columns. The mechanical property of each component is reported in the aforementioned reference. The yield stress and stress-strain curves were extracted and defined to the software for each element. P- Δ effect is considered in the analysis. The load-displacement curve of the first floor extracted from the experimental hysteresis curve is compared to the obtained numerical one in Figure 4b. As it can be seen, there is a good accordance.

Numerical Modeling of Cracked Plate

To validate the crack growth process modeling, an experimental test program (Simonsen and Tornqvist, 2004) was considered as illustrated in Figure 5.

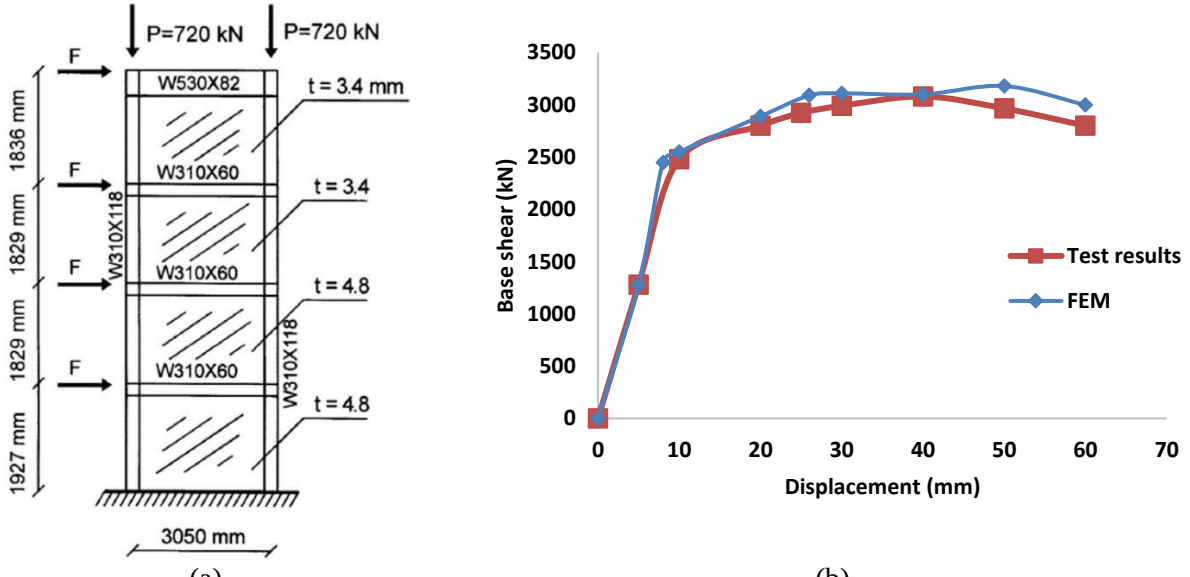

Fig. 4. Steel Plate shear wall system without crack: a) Test setup (Driver, 1998), b) Load–displacement response

The case is a thin steel plate with an edge crack of 300 (mm) loaded in mode I with a displacement-control fashion. The elastic modulus and Poisson's ratio of the material are 210 GPa and 0.30, respectively. The maximum principal stress criterion and the energy criterion based on the standard exponential law were used as crack initiation and crack growth criteria. The XFEM method as described in before was used to estimate the crack growth.

During the testing, the crack length increased approximately 350 mm that was calculated around 348 mm in FE modeling. In addition, The FE modeling showed a good estimation to crack propagation as illustrated in Figure 6. The displacement of two edges of crack has shown exaggeratedly to show the crack opening and crack propagation. Moreover, the calculated curve for crack propagation and plastic strain, respectively, against the displacement is shown in Figure 7, which is good coinciding with the one reported in the aforementioned reference.

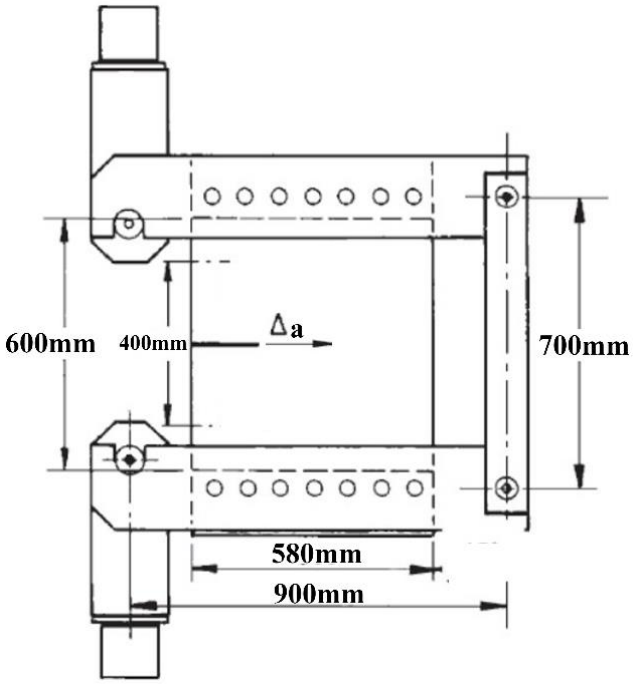

Fig. 5. Test setup (Simonsen and Tornqvist, 2004)

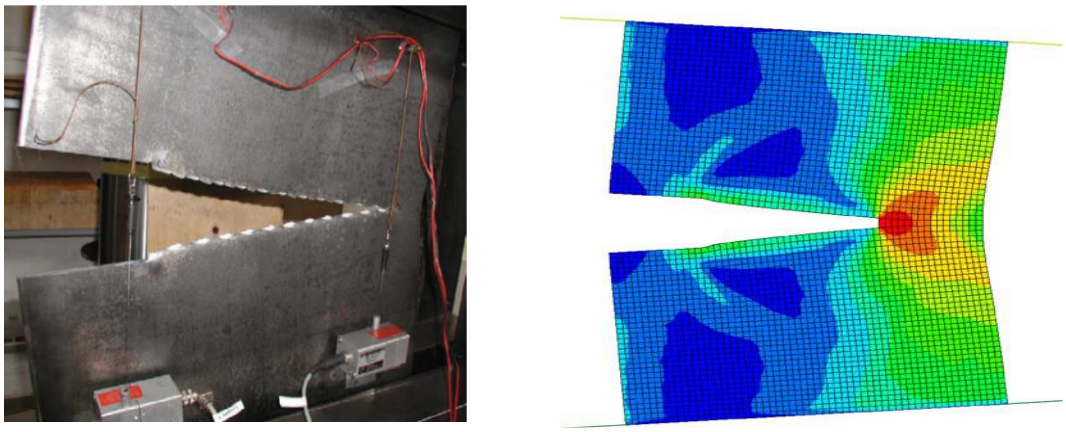

Fig. 6. Comparing of experimental with FE modeling; crack opening

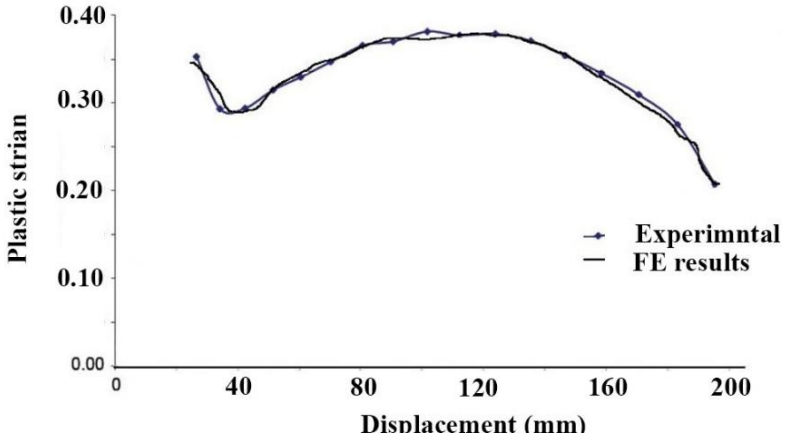

Fig. 7. Comparing the test results with FE modeling

NUMERICAL MODELING

Specifications of Steel Shear Wall Models

Table 1 shows the specifications of the models considered in this study to investigate the effect of initial position of crack and also the effect of crack growth on the SPSW behavior. In all the models, the steel plate has a thickness of 4mm and L = 4 m and h = 3 m. The label of each model consists of three characters and a number. The first letter in the future curves can be S, P or F representing the SPSW, Plate of SPSW and Frame of SPSW, respectively. The second character can be 2C, 2T, … standing for cracks location as in Figure 2. The numeric part represents the crack length in centimeters. For example, "S-2C-7.5" is a steel plate shear wall with a crack at compressive diagonal with an initial crack length of 7.5 cm.

The SPSW is designed according to the AISC Design Guide 20 (AISC, 2007) and the AISC 360-10 (AISC, 2010) rules and provisions. The SPSW is designed by the following capacity-design principles so that the infill plate is assumed to resist forces corresponding to its expected full shear yield strength. HBEs and VBEs are designed to allow the formation of full yield lines across the plate, to resist the corresponding forces from the infill, and to remain elastic. Plastic hinges are only allowed to form at the ends of HBEs and lower ends of VBEs. In this way, the system would maintain stability even after yield zones propagate across the infill plate. The designed sections for HBEs and VBEs are W14 × 176 and W14 × 257, respectively as shown in Figure 8. Typical models have shown in Figure 9 for FE modeling in ANSYS and ABAQUS.

Material Properties

The ST37 steel is considered here. Young modulus is 210 GPa and Poisson ratio is assumed to be 0.3. The ST37 steel has a good machinability and surface finish capabilities with a high strength and adequate workability. Reference mechanical properties are summarized in Table1. Material flow curve for steel ST37 at room temperature is described using a power law. Power law is usually a suitable approximation of plastic response curve.

$$\sigma = A + B\varepsilon_p^m \quad (10)$$

where three parameters A, B, and m need to be determined. The Von-Mises yield criterion, known to be the most suitable yield function for metals, is used in this research. The type of hardening to be used in this simulation is isotropic hardening. And also, the parameters of power law based on Bonora damage model parameters for this material (Bonora, 2006) is given in Table 2, and flow curve diagram is depicted in Figure 10.

Table 1. Model properties

Model	2a (cm)	Crack Type	Initial Crack Position (Figure 2)
S-2C-7.5	7.5	Horizontal	2C
S-2C-15	15	Horizontal	2C
S-2C-30	30	Horizontal	2C
S-2C-60	60	Horizontal	2C
S-2C-120	120	Horizontal	2C
S-2C-240	240	Horizontal	2C
S-2T-7.5	7.5	Horizontal	2T
S-2T-15	15	Horizontal	2T
S-2T-30	30	Horizontal	2T
S-2T-60	60	Horizontal	2T
S-2T-120	120	Horizontal	2T
S-2T-240	240	Horizontal	2T
S-3C-7.5	7.5	Horizontal	2T
S-3C-15	15	Horizontal	3C
S-3C-30	30	Horizontal	3C
S-3C-60	60	Horizontal	3C
S-3C-120	120	Horizontal	3C
S-3C-240	240	Horizontal	3C
S-3T-7.5	7.5	Horizontal	3C
S-3T-15	15	Horizontal	3T
S-3T-30	30	Horizontal	3T
S-3T-60	60	Horizontal	3T
S-3T-120	120	Horizontal	3T
S-3T-240	240	Vertical	3T
S-4C-7.5	7.5	Vertical	4C
S-4C-15	15	Vertical	4C
S-4C-30	30	Vertical	4C
S-4C-60	60	Vertical	4C
S-4C-120	120	Vertical	4C
S-4C-240	240	Vertical	4C
S-4T-7.5	7.5	Vertical	4T
S-4T-15	15	Vertical	4T
S-4T-30	30	Vertical	4T
S-4T-60	60	Vertical	4T
S-4T-120	120	Vertical	4T
S-4T-240	240	Vertical	4T
S-5C-7.5	7.5	Vertical	4T
S-5C-15	15	Vertical	5C
S-5C-30	30	Vertical	5C
S-5C-60	60	Vertical	5C
S-5C-120	120	Vertical	5C
S-5C-240	240	Vertical	5C
S-5T-7.5	7.5	Vertical	5C
S-5T-15	15	Vertical	5T
S-5T-30	30	Vertical	5T
S-5T-60	60	Vertical	5T
S-5T-120	120	Vertical	5T
S-5T-240	240	Vertical	5T

Table 2. ST37 steel properties

Flow curve Parameters			**Damage Parameters**				
A (MPa)	B (MPa)	m	ε_{th}	ε_f	D_0	D_{cr}	α
217	233.7	0.6428	0.259	1.4	0.0	0.065	0.2175

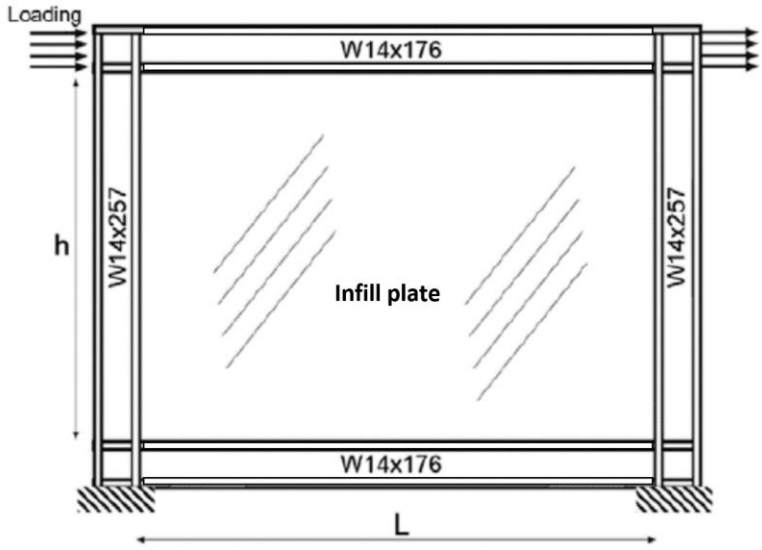

Fig. 8. A typical SPSW system

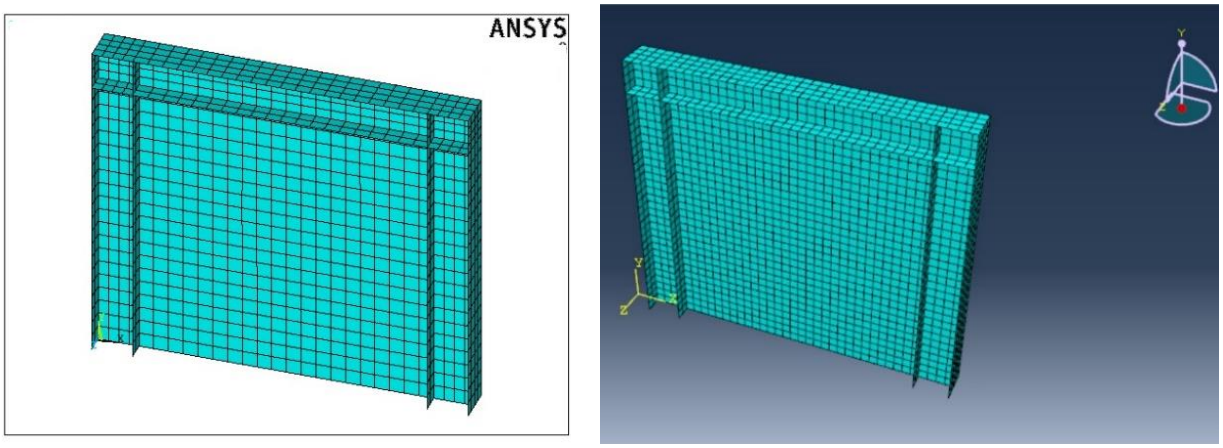

Fig. 9. A typical FE models in ANSYS and ABAQUS

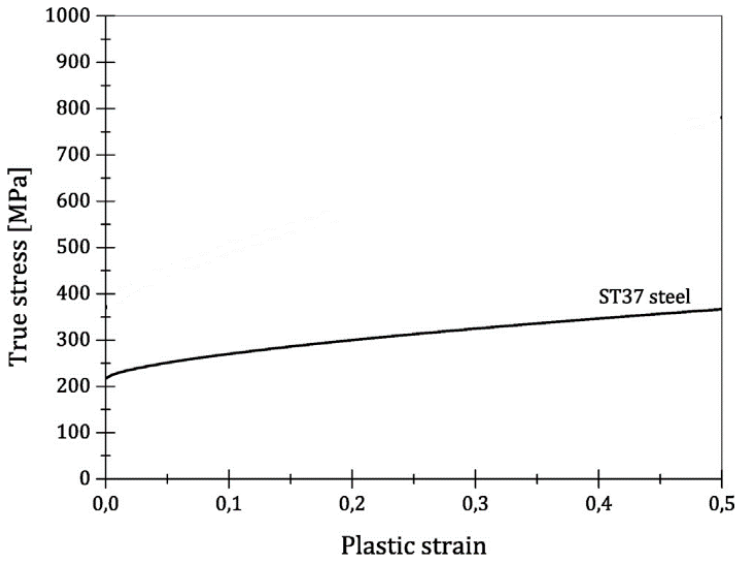

Fig. 10. Typical tensile curve for ST37 steel

The maximum principal stress criterion and the energy criterion based on the standard exponential law were used as crack initiation and crack growth criteria. Yield strength and fracture energy are assumed as 220 MPa and 42.2 N/mm, respectively.

Loading and Boundary Conditions

Lateral loads are applied to the beam-column connections as shown in Figure 10; and are gradually increased from zero to a magnitude beyond the system's capacity. The ultimate displacement limit is considered to occur at a drift ratio of 2.5% per ASCE 7-05 (ASCE, 2010). To simulate the fixed condition of the column-to-base plate connections, the bottom nodes of both columns flanges and webs are restrained from displacement in all directions. To simulate the constraints imposed by slabs of the story floors, the out-of-plane displacements of beam webs are also restrained.

Defining the Seismic Behavior Parameters

In order to estimate seismic parameters, the actual load-displacement response curves are usually idealized as illustrated in Figure 11. This idealization is based on the following assumptions and definitions:

- The maximum displacement of the structure, Δ_{max}, will be considered based on the requirements of the local regulations.
- The Ductility factor is measured as $\mu = \Delta_{max} / \Delta_y$ from ideal curve.
- The elastic stiffness, K, is equal to initial slope of the load-deformation curve; $= \frac{V_y}{\Delta_y}$.
- The over strength factor, Ω, factor is the reserved strength value existing between V_y and V_s.
- Response modification factor is determined as $R = V_e / V_s$

RESULTS AND DISCUSSION

Load-Displacement Curve

Load-displacement curve contains important information, and seismic parameters can be extracted from it. Figures 12 and 13 show the load-displacement curve for walls containing horizontal or vertical cracks with fixed lengths (without considering the crack growth phenomenon).

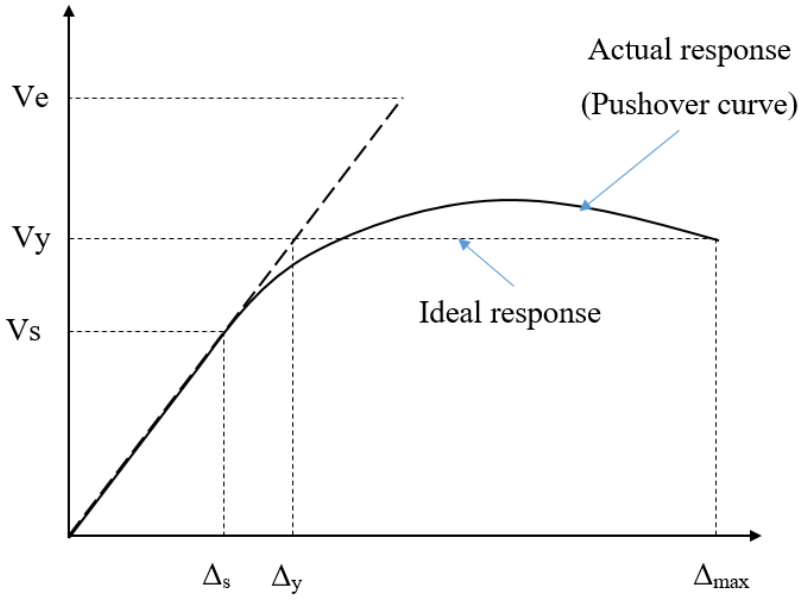

Fig. 11. Idealization of load–displacement curve of structures

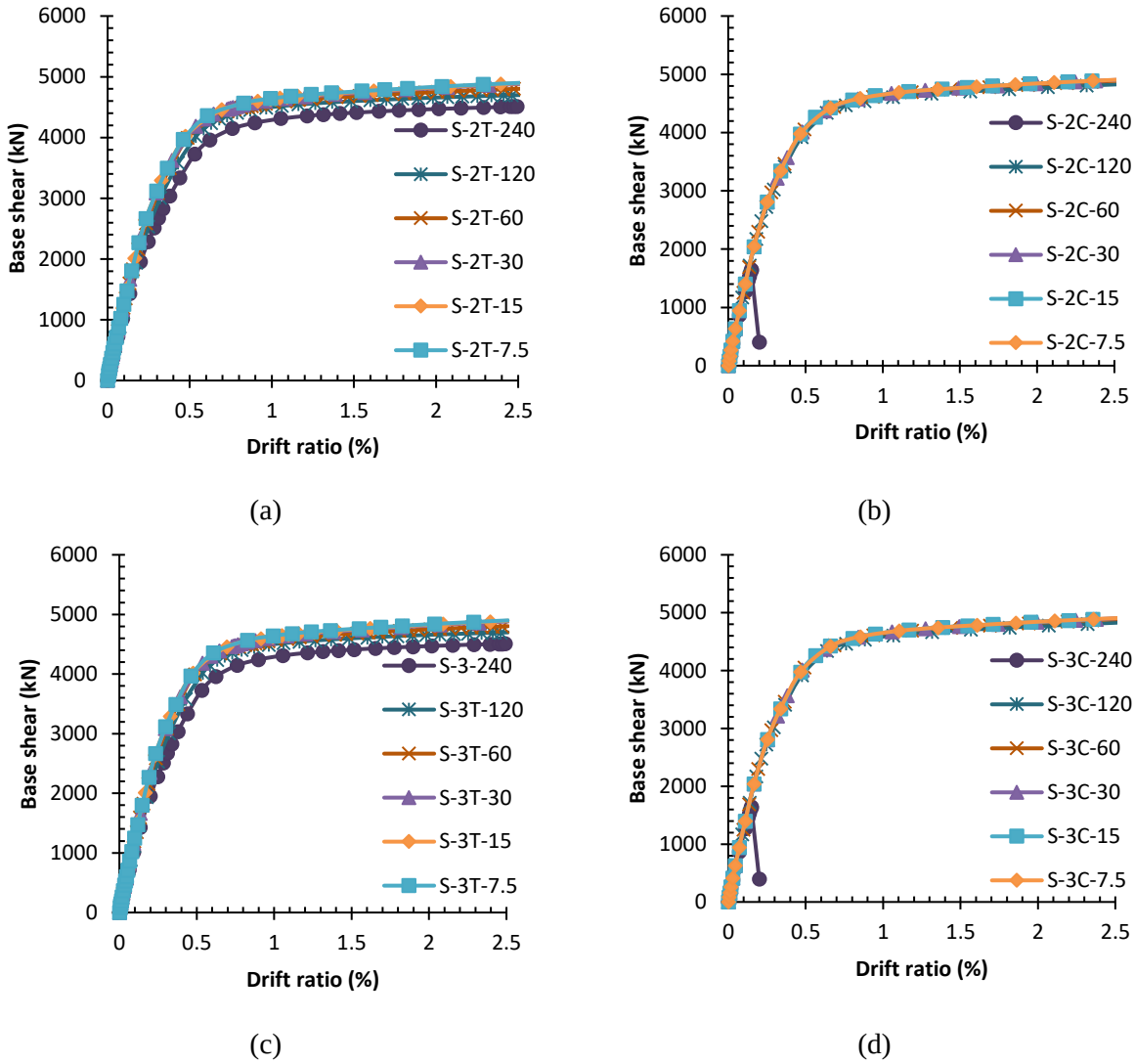

Fig. 12. Load-displacement of cracked SPSW with vertical crack, initial crack at; a) 2T, b) 2C, c) 3T, 3C

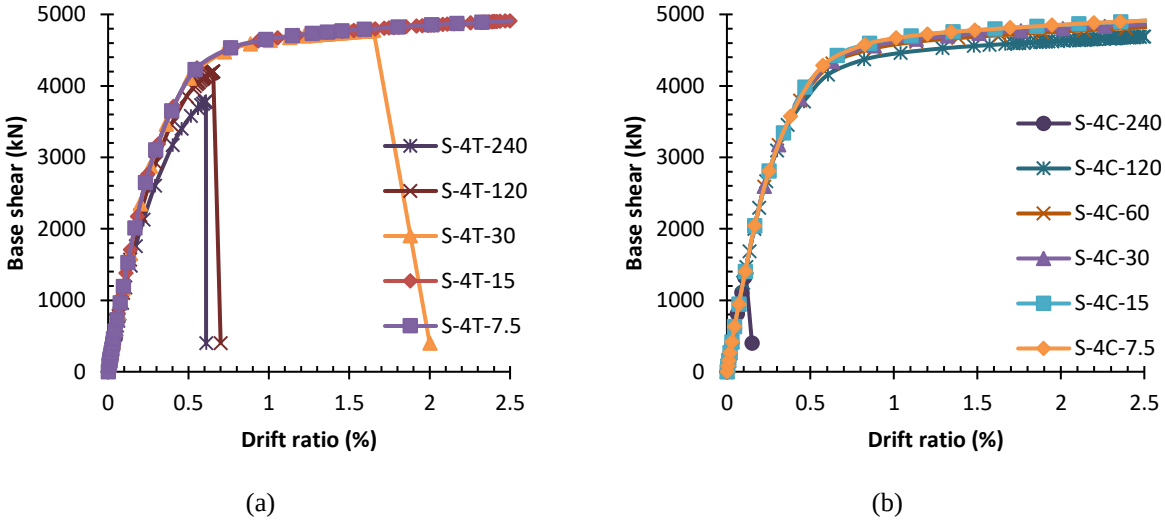

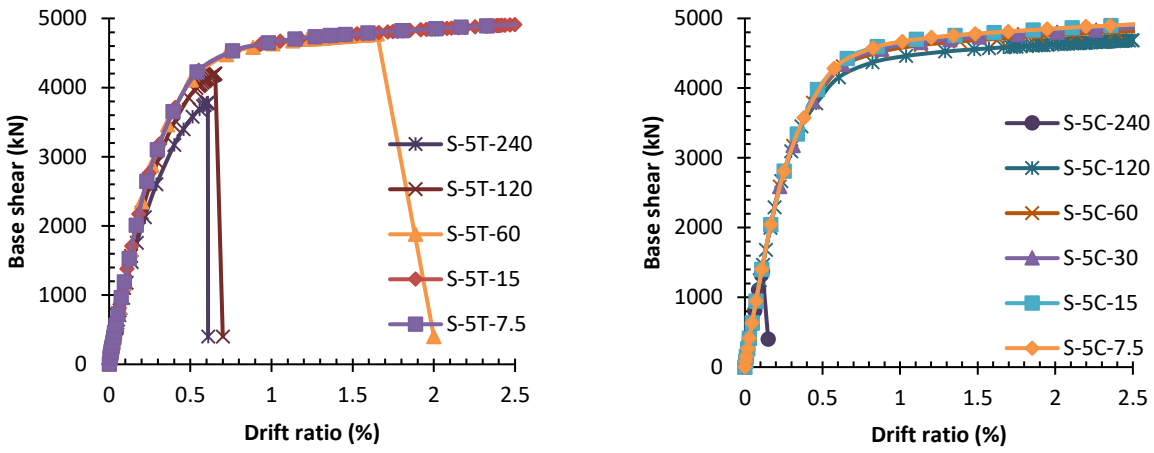

(c) (d)

Fig. 13. Load-displacement of cracked SPSW with horizontal crack, initial crack at a) 4T, b) 4C, c) 5T, d) 5C

The figures show that, the cracked shear wall of 2 with 3 and also 4 with 5 have the same behavior. In all models, crack located at the tension diagonal field of plate (models including T letter name) decreases the strength and energy absorption more than crack on the compressive diagonal (models including C letter name). Despite vertical cracks (models S-4 and S-5), the horizontal cracks (models S-2 and S-3) could have a great impact on the nonlinear behavior of SPSW, Figure 13. For horizontal cracks with a length of more than 300 mm, the wall ruptures suddenly and for cracks longer than 1200 mm, the wall system is ruptured low entering the nonlinear phase. This means that the wall with such a crack cannot be considered as a load-bearing ductile system. Therefore, it can be inferred that horizontal cracks are more critical than vertical cracks. This phenomenon may be related to the location of diagonal tension field burden of load bearing.

Wall-Frame Shares of Story Shear

An alternative method to evaluate the effectiveness of infill plates is to measure the amount of absorbed story shear. The curves presented in Figure 14, illustrate the amount of shear forces carried by the infill plate in various SPSWs having different initial cracks. Figure 14, on the other hand, shows the percentage contribution shares of the infill plates at different drift ratio. The absorbed shear forces are calculated by means of integrating shear stresses across the width of infill plates. Figure 15 shows a very high contribution from the infills up to a drift ratio of around 0.5%, where the surrounding members experience their first yield points. Thereafter, the curves start to rise a little until that becomes horizontal at around the drift ratio of 1.2%. Beyond the drift ratio of 1.2%, the surrounding members mainly absorb additional loading. It should be noted that, due to the high in-plane strength of infill plates, the load bearing capacity corresponding to the drift ratio of 1.2% is very close to the ultimate strength of the system. In first stage of loading, the share of infill plate is around 65% whereas in drift ratio 0.5% decreases to around 40%. Reduction of share of infill plate from lateral load for bigger initial crack is more than initial crack, and also this reduction is more for horizontal small initial crack comparison to vertical initial cracks.

Figure 15 also shows that the infill plates are very active during the initial stages of loading and absorbs a major part of the story

shear. The curves in Figure 16 indicate that the contribution share of the infill plates is almost constant until the formation of diagonal yield zones. After the development of diagonal yield zones, the contribution of shear infill plates gradually decreases and after the drift ratio of 1.2%, that becomes almost constant. This noted is true when tearing of infill plate does not occur. On other hand, the walls with long initial crack do experience this process, especially initial horizontal crack (models with Crack No. 4 and 5).

Figures 16a,b illustrate the contribution shares of the infill plates and frames during the loading history of SPSW models. The figure shows that the infill plates absorb a high percentage of story shears at the early stages of loading. Upon the formation of diagonal yield zones, the plates begin to lose their effectiveness and frames become more active. Again, after the drift ratio of 0.2%, the frame and infill plats absorb almost constant shares of loading. It should be mentioned that the yield zones in the infill plates are very narrow at the beginning; but gradually widen to almost the entire surface of the wall. Referring to Figures 16c,d, it can be seen that initial vertical crack does not have significant effect on shares of the infill plates and frame during the loading history for drift ratio higher than 1.2%. Nevertheless, in SPSWs with horizontal crack, the initial crack leads the wall to reduce the infill plate sharing.

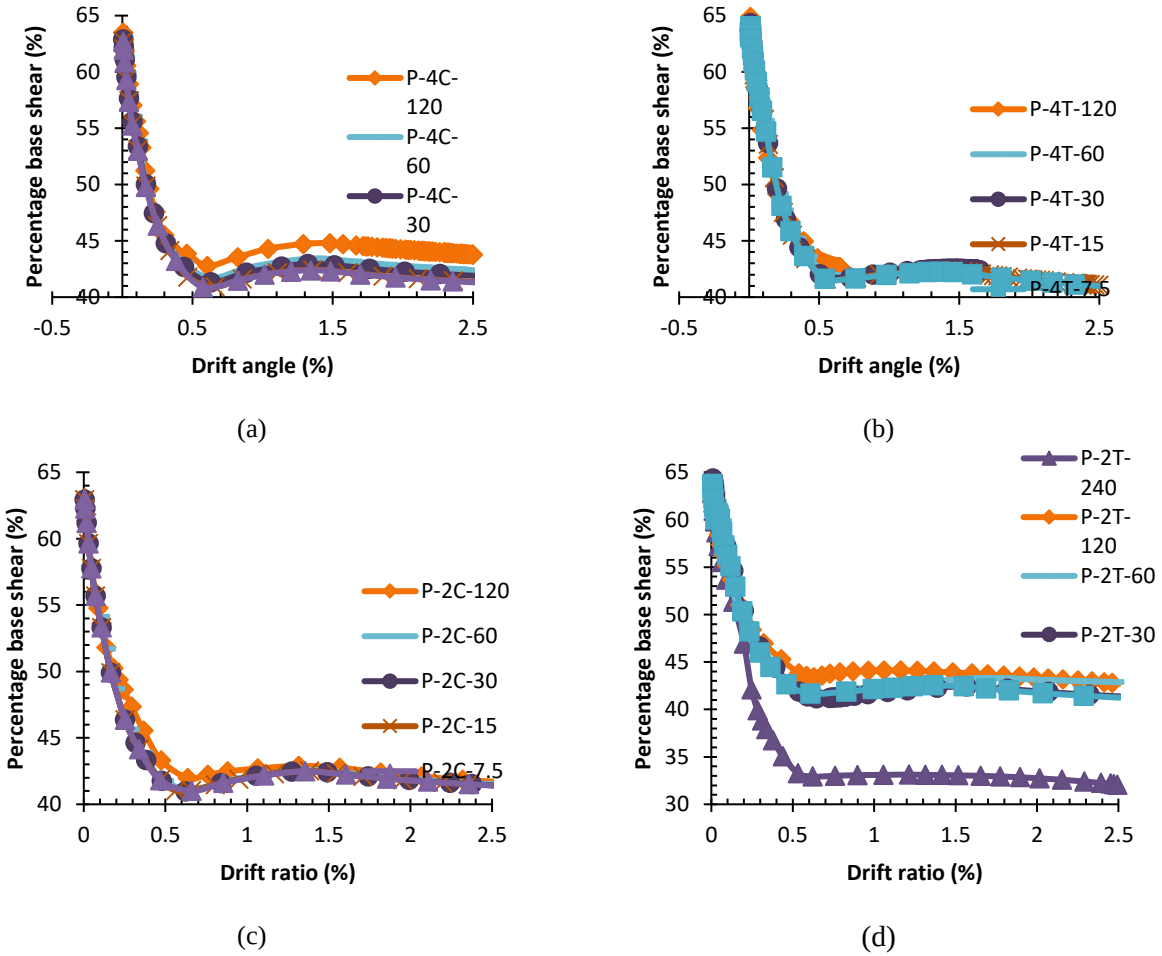

Fig. 14. Percentage share of story shear by the infill plates; a) Cracks No. 4C, b) Cracks No. 4T, c) Cracks No. 2C, d) Cracks No. 2T

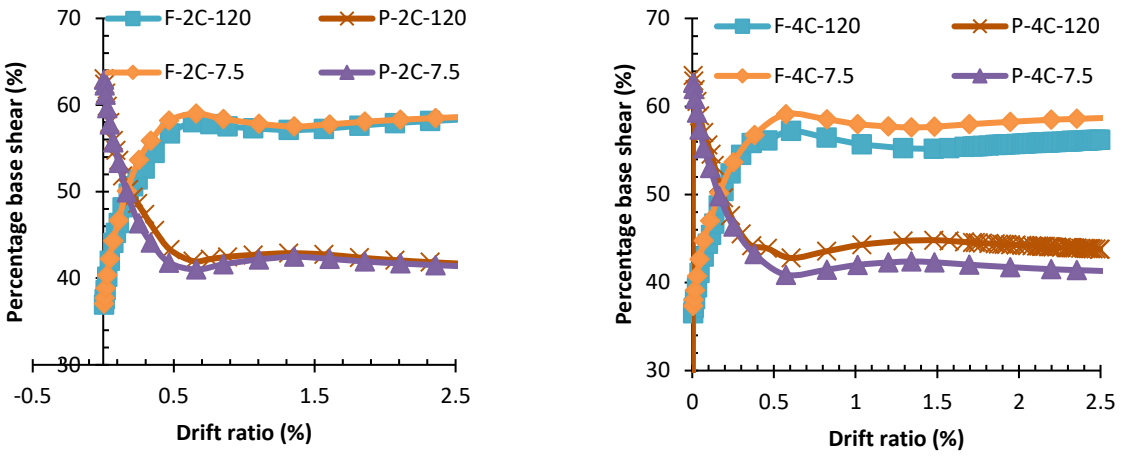

models crack No. 2 models crack No. 4

Fig. 15. Percentage shear intakes by the infill and frame for small and long crack

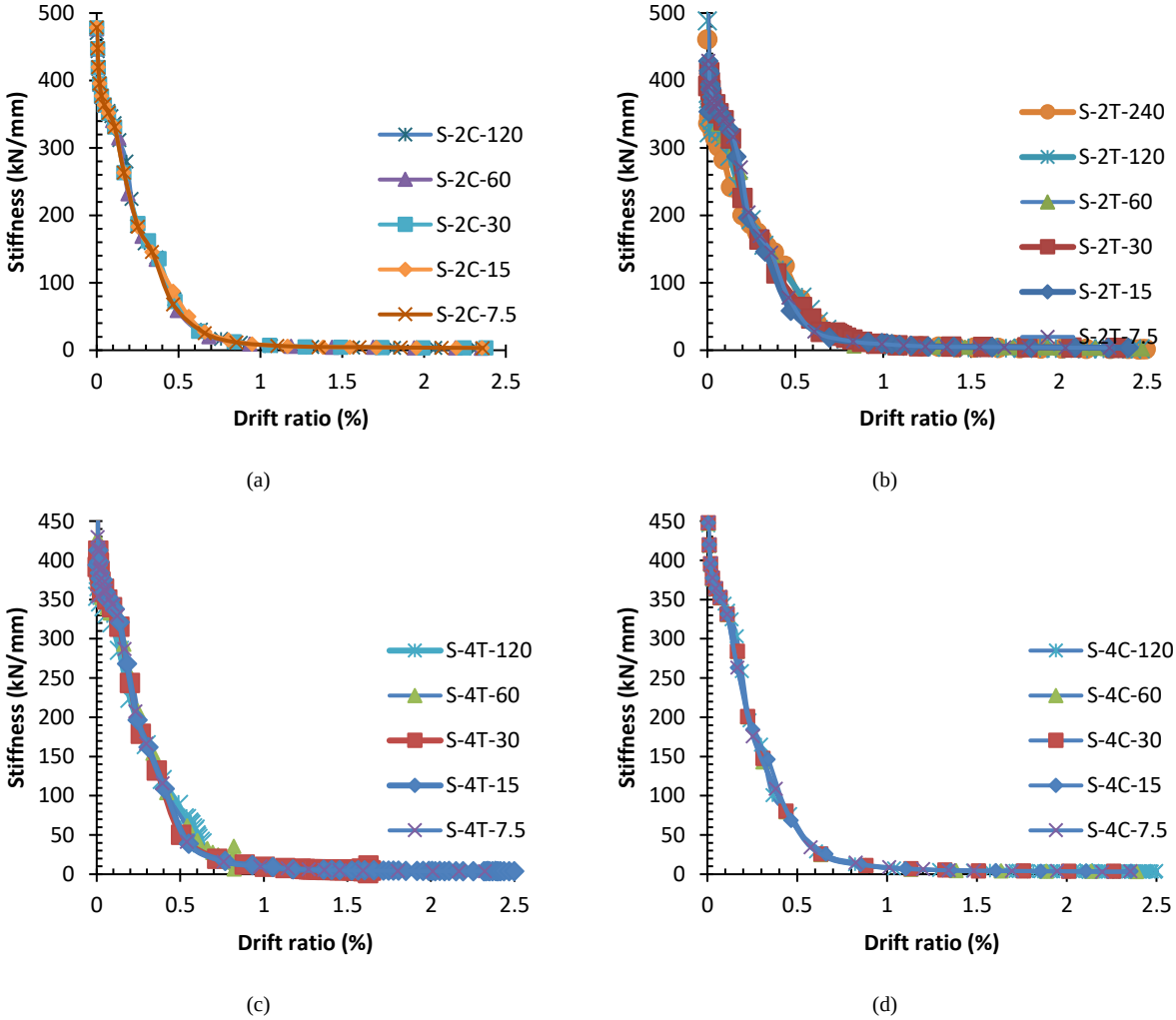

Fig. 16. Stiffness-Drift curve: a) S-2C models, b) S-2T models, c) S-4T models, d) S-4C models

Frame members of the bays containing infill plates must provide adequate boundary conditions for the plates to ensure full yielding across the wall. Otherwise, only a limited band in the wall plastifies prior to the formation of plastic hinges in frame members, and the system becomes less ductile. However, after the development of first yield points in the frame members, the system gradually loses its efficiency to withstand further stresses. In addition, once plastic hinges are formed in the frame members, the magnitude of stresses within the plate remains constant. From the seismic design point of view, minor earthquake loads can be dissipated by the infill plates by undergoing small inter-story drifts (< 0.1%). In moderate earthquakes, the infill plates experience widespread yielding, while the frame members remain elastic. This is an ideal choice since the structures remain in the state of immediate occupancy, and if necessary, the infill plates are easily repairable. Under severe earthquakes, however, the structure dissipates noticeable energy, and plastic hinges are formed in frame members. The structures may suffer minor damages; but due to the high ductility, they do not collapse.

Stiffness and Strength

Two parameters that are important in elastic and inelastic zone are lateral stiffness and lateral strength. Lateral stiffness curves are utilized to measure the contribution share of infill plates in both resisting the lateral loads. The reduction of stiffness increases P-Δ effect. In addition, Low amount of shear strength increases the ductility demand and possibility of structure demolition.

The stiffness curves of SPSWs with crack No. 2 (and No. 3 is same as to it) and crack No. 4 (and Crack No. 5 is same as to it) and various infill initial crack length are given in Figure 16. It should be noted that increasing the initial crack decreases the initial lateral stiffness, Table 3. Nevertheless, after the appearance of diagonal yield zones, which incidentally occur at similar drift ratios, the curves tend to converge towards each other.

Table 3. Ductility, initial stiffness, ultimate strength of SPSW

Models	μ	Fu (kN)	K (kN/mm)
S-2C-7.5	8.3	4906.38	478.89
S-2C-15	8.29	4906.42	478.79
S-2C-30	8.29	4903.2	478.31
S-2C-60	8.29	4888.65	476.85
S-2C-120	8.29	4826.63	470.71
S-2C-240	Elastic behavior	1645.1	438.36
S-2T-7.5	8.75	4900.26	504.61
S-2T-15	8.76	4893.68	504.44
S-2T-30	8.77	4882.03	503.63
S-2T-60	8.86	4802.87	500.86
S-2T-120	8.84	4698.89	488.84
S-2T-240	8.69	4509.38	461.13
S-4C-7.5	7.75	4914.83	447.86
S-4C-15	7.75	4912.92	447.74
S-4C-30	7.83	4860.158	447.53
S-4C-60	7.89	4817.97	446.97
S-4C-120	Elastic behavior	3092.42	444.29
S-4C-240	Elastic behavior	1372.98	427.08
S-4T-7.5	7.43	4912.82	429.41
S-4T-15	7.43	4910.26	429.41
S-4T-30	7.02	4770.46	393.74
S-4T-60	7.39	4507.33	391.61
S-4T-120	Around elastic behavior	4200.53	428.43
S-4T-240	Around elastic behavior	3782.47	354.10

It is also observed that with the increase of initial crack, the plateau between the first yield and diagonal yield zones of the walls fades away, and the system experiences sharper loss of stiffness. After the occurrence of the first yield points in frame members and between the drift ratios of 0.5% and 1%, infills become less effective and all stiffness curves merge to the open frame curve, it is highlighted in the C models than T models. In other words, after the drift ratio of 1%, it is only the frame that carries lateral loads. So, initial crack does not have considerable effect on stiffness of walls.

The calculated initial stiffness and ultimate strength of cracked SPSWs are listed as shown in Table 3. As it can be seen, small initial crack length has very little effect on the initial stiffness and ultimate strength of systems. However, for cracks longer than 600 mm, both parameters show a significant decrease.

The results also demonstrate that the infill plates generally have their first yield at a drift ratio of around 0.1%. With the propagation of yield zones, beam ends and bottom of columns plastify at a drift ratio of around 1%. Top of columns, however, remain essentially elastic due to the ``weak beam-strong column" design criteria. Therefore, enough time is available to the system to develop widespread plasticity before plastic hinges are formed in the beams and columns. This is to meet the capacity-design principles as stated in the AISC design codes (AISC, 2007; AISC, 2010) that system ductility shall be primarily provided by plastic deformation of the infill plates. Table 1 shows the measured ductility of SPSWs with different initial cracks. The ductility is calculated as depicted in Figure 12. Based on the results given in Table 1, the ductility of the SPSWs is almost independent of the initial crack in T or C zones but decreases with the horizontal crack (crack No. 4) more than vertical cracks (models with crack No. 2). It should be noted that when the initial crack is bigger than 1200 mm, system has an elastic behavior that the ductility is not defied.

Energy Absorption

One of the accurate ways of measuring seismic performance of a structure relies on energy dissipation. The structures with higher capability in energy absorption can be designed for smaller lateral forces. In the present paper, the dissipated energy of analyzed specimens is measured as the area enclosed by load−displacement curve.

It can be seen with referring to the Table 4 and Figure 17 that by increasing the crack length, the energy absorption of system is decreased. Decreasing of energy absorption capability in models with cracks T types is much more than models with cracks C types.

This table shows that decreasing of energy absorption due to small initial crack is negligible. Energy absorption decreasing of all models for T zone is little more than C zone. Nevertheless, there is a considerable difference between cracks No. 2 and cracks No. 4 especially in T zones. The critical crack is the crack on the T zones with length more than 1.8% of the weld length. Table 4 compares energy absorption for walls with central cracks. This comparison is obvious because energy absorption of system has a significant reduction of 0.9% to 79%.

Response Modification Factor (R Factor)

The calculated response modification factors along with their components for the wall with various cracks are listed in Table 5. It shows that if there is a small crack only in Fishplate connected to column (vertical crack), the cracked steel shear walls can be used in areas with high seismic risk and ductile behavior expectation. Walls containing horizontal cracks with a length of nearly 15% of the wall plate can be used only in low seismic risk areas and low ductility expectation. For bigger cracks, the wall

cannot be regarded as a system of load bearing seismic system since its behavior is limited to the elastic region. It should be noted that all these conclusions were drawn with the assumption of non-growing crack. According to the Table 5, sensitivity of the Ru factor is based on horizontal crack than vertical initial cracks. But, horizontal cracks reduce the Ru factor. Cracks with a length of less than 15% of the wall length have little effect on the R_μ factor. Based on the results given in Table 5, the R_μ of the SPSWs is almost independent of the initial crack length of the wall. Slight decreases of response modification factor are derived from the horizontal cracks.

Table 4. Ductility, initial stiffness, ultimate strength of SPSW

	Initial Crack Length (mm)	**75**	**150**	**300**	**600**	**1200**	**2400**
Crack No. 2	C zone	363.26	363.53	363.19	362.04	358.01	4.44
	Decreasing compared to S-75 (%)	100	100	100	100	99	1
	T zone	363,05	362.04	361.06	356.64	348.88	331.60
	Decreasing compared to S-75 (%)		100	99	98	96	91
Crack No. 4	C zone	363.73	363.87	360.16	357.44	297.85	2.71
	Decreeing compared to S-75 (%)	1.00	1.00	0.99	0.98	0.82	0.01
	T zone	363.79	333.22	221.21	90.86	61.13	49.49
	Decreasing compared to S-75 (%)	100	92	61	25	17	14
Models with cracks T dived to cracks C	Crack No. 2	1.00	1.00	0.99	0.98	0.97	82.9
	Crack No. 4	1.00	0.91	0.62	0.25	0.21	20

Table 5. Modification factor

	R_μ	Ω	R_u
S-2C-7.5	3.8	1.75	6.64
S-2C-15	3.8	1.75	6.65
S-2C-30	3.8	1.75	6.64
S-2C-60	3.8	1.64	6.25
S-2C-120	3.8	1.77	6.74
S-2C-240		Elastic behavior	
S-2T-7.5	3.91	1.84	7.18
S-2T-15	3.91	1.85	7.23
S-2T-30	3.91	1.8	7.02
S-2T-60	3.94	1.85	7.30
S-2T-120	3.93	1.86	7.29
S-2T-240	3.88	1.98	7.67
S-4C-7.5	3.67	1.75	6.43
S-4C-15	3.67	1.75	6.43
S-4C-30	3.69	1.88	6.93
S-4C-60	3.71	1.86	6.91
S-4C-120		Elastic behavior	
S-4C-240		Elastic behavior	
S-4T-7.5	3.6	1.75	6.3
S-4T-15	3.45	1.75	6.03
S-4T-30	2.77	1.84	5.09
S-4T-60	1.87	1.74	3.26
S-4T-120		Elastic behavior	
S-4T-240		Elastic behavior	

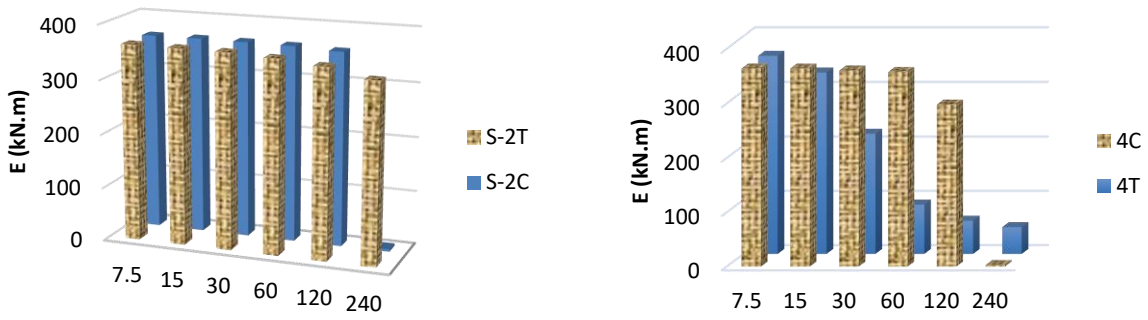

(a) (b)

Fig. 17. Energy absorption of wall with; a) Cracks No. 2, b) Cracks No. 4

Comparison of Horizontal and Vertical Crack

To evaluate the effect of crack type in the case of non-growing condition, the seismic parameters of the walls with horizontal and vertical crack are listed in Table 6. The results reveal that in long cracks, the horizontal cracks are more critical than the vertical cracks. The main reason is the failure of wall with horizontal crack in the elastic region. In the shorter edge cracks, stiffness, strength and energy absorption has a greater amount.

CONCLUSIONS

In the present work, the effect of crack on the seismic behavior of SPSW was investigated and the following results are briefly concluded:

- The results revealed that the horizontal cracks located on the top or bottom of SPSW have the same effect. In addition, it is the case for the vertical cracks located at the left or right of SPSW. Moreover, the horizontal cracks (models S-2 and S-3) could have a great impact on the nonlinear behavior of SPSW in spite of the vertical cracks (models S-4 and S-5).
- In all the models, the cracks located at the tension diagonal field of plate (models including "T" in their name) decrease the strength and energy absorption more than the crack on the compressive diagonal (models including "C" in their name). The critical crack is the crack on the T zones with length more than 1.8% of the weld length. These cracks reduce 0.9% to 79% of the energy absorption of system. Energy absorption decreasing of all models for T zone is a little more than C zone. However, there is a considerable difference between cracks No. 2 and cracks No. 4 especially in T zones.

Table 6. Comparison of vertical crack and horizontal crack

Crack No. 4 Divided to Crack No. 2	Initial Crack Length (mm)	75	150	300	600	1200	2400
E	C zone	1.00	1.00	0.99	0.99	0.83	0.61
	T zone	1.00	0.92	0.61	0.25	0.18	0.15
K	C zone	0.94	0.94	0.94	0.94	0.94	0.97
	T zone	0.85	0.85	0.78	0.82	0.88	0.81
Fu	C zone	1.00	1.00	0.99	0.99	0.64	0.83
	T zone	1.00	1.00	0.98	0.96	0.89	0.80

- Frame members of the bays containing infill plates must provide adequate boundary conditions for the plates to ensure full yielding across the wall. Otherwise, only a limited band in the wall plastifies prior to the formation of plastic hinges in frame members and the system becomes less ductile. In addition, the results also demonstrate that the infill plates generally have their first yield at a drift ratio of around 0.1%. With the propagation of yield zones, beam ends and the bottom of columns become plastic at a drift ratio of around 1%.
- With the increase of initial crack, the plateau between the first yield and diagonal yield zones of the walls fades away, and the system experiences sharper loss of stiffness. After the occurrence of the first yield points in frame members and between the drift ratios of 0.5% and 1%, infills become less effective and all stiffness curves merge to the open frame curve, it is more highlight in the C models than T models. In other words, after the drift ratio of 1%, it is only the frame that carries lateral loads. Therefore, initial crack does not have considerable effect on stiffness of walls.

REFERENCES

Abdollahzadeh, G.R., Kuchakzadeh, H. and Mirzagoltabar, A.R. (2017). "Performance-based plastic design of moment frame-steel plate shear wall as a dual system", *Civil Engineering Infrastructures Journal*, 50(1), 21-34.

Abdollahzadeh, G. and Malekzadeh, H. (2013). "Response modification factor of coupled steel shear walls", *Civil Engineering Infrastructures Journal*, 46(1), 15-26.

AISC. (2007). *Steel design guide 20, steel plate shear walls, Chicago (IL)*, American Institute of Steel Construction, Chicago.

AISC, ANSI/AISC 341-10, (2010). *Seismic provisions for structural steel buildings*, American Institute of Steel Construction.

Alinia, M., Hosseinzadeh, S. and Habashi, H. (2007). "Numerical modelling for buckling analysis of cracked shear panels", *Thin-walled Structure,* 45, 1058–1067.

ANSYS. (2016). *User manual*, ANSYS, Inc., Canonsburg, PA.

ASCE, SEI/ASCE 7-10. (2010). *Minimum design loads for buildings and other structures*. American Society of Civil Engineers. Virginia.

Astaneh-Asl, A. (2001). *Seismic behavior and design of steel shear walls*, S.S.E. Council, California.

Basler, K. (1961). "Strength of plate girders in shear", *Journal of Structural Division*, ASCE, 128, 683-719.

Belytschko, T., Chen, H., Xu, J. and Zi, G. (2003). "Dynamic crack propagation based on loss of hyperbolicity and a new discontinuous enrichment", *International Journal for Numerical Methods in Engineering*, 58, 1873-1905.

Bert, C. and Devarakonda, K. (2003). "Buckling of rectangular plates subjected to nonlinearly distributed in-plane loading", *International Journal of Solids and Structures*, 40, 4097-4106.

Bonora, N, (2006). "A nonlinear CDM model for ductile failure", *Engineering Fracture Mechanic*, 58, 11-28.

Brighenti, R. (2005). "Buckling of cracked thin-plates under tension or compression", *Thin-Walled Structures,* 43, 209-224.

Broujerdian, V., Ghamari, A. and Ghadami, A. (2016). "An investigation into crack and its growth on the seismic behavior of steel shear walls", *Thin-Walled Structures*, 101, 205-212.

Campilho, R., Banea, M., Chaves, F. and Da-Silva, L. (2011). "Extended Finite Element method for fracture characterization of adhesive joints in pure mode I", *Computational Materials Science*, 50, 1543-1549.

Driver, R., Kulak, G., Kennedy, D. and Elwi, A. (1998). "Cyclic test of four-story steel plate shear wall", *Journal of Structural Engineering*, 124, 112-120.

Dubina, D., and Dinu, F. (2014). "Experimental evaluation of dual frame structures with thin-walled steel panels", *Thin-Walled Structures*, 78, 57-69.

Golewski, G., Golewski, P., and Sadowski, T. (2012). "Numerical modelling crack propagation under Mode II fracture in plain concretes containing siliceous fly-ash additive using XFEM method", *Computational Materials Science*, 62, 75-78.

Guendel, M., Hoffmeister, B. and Feldmann, M. (2011). "Experimental and numerical investigations on steel shear walls for seismic retrofitting", *Proceedings of the 8th International Conference on Structural Dynamics*, Belgium.

Hatami, F., Ghamari, A. and Rahai, A. (2012). "Investigating the properties of steel shear walls reinforced with carbon fiber polymers (CFRP)",

Journal of Constructional Steel Research, 70, 36-42.

Hibbitt, H., Karlsson, B. and Sorensen, P. (2012). *ABAQUS theory manual, version 6.12*, Pawtucket, Rhode Island, USA.

Johnson, G.R., and Cook, W.H. (1983), "A constitutive model and data for metals subjected to large strains, high strain rates and high", *Proceedings of the 7th International Symposium on Ballistics*, 21, 541-547

Nasirmanesh, A. and Mohammadi, S. (2017). "Eigenvalue buckling analysis of cracked functionally graded cylindrical shells in the framework of the extended Finite Element method", *Composite Structures*, 159, 548-566.

Riks, E., Rankin, C. and Brogan, F. (1992). "The buckling behavior of a central crack in a plate under tension", *Engineering Fracture Mechanics*, 43, 529-548.

Shaw, D. and Huang, Y. (1990). "Buckling behavior of a central cracked thin plate under tension", *Engineering Fracture Mechanics*, 35, 1019-1027.

Shekastehband. B., Azaraxsh. A. and Showkati. H, (2017), "Experimental and numerical study on seismic behavior of LYS and HYS steel plate shear walls connected to frame beams only", *Archives of Civil and Mechanical Engineering*, 17(1),154-168.

Sih, G. and Lee, Y. (1968). "Tensile and compressive buckling of plates weakened by cracks", *Theoretical and Applied Fracture Mechanics*, 6, 129-138.

Simonsen, B. and Tornqvist, R. (2004). "Experimental and numerical modelling of ductile crack propagation in large-scale shell structures", *Marine Structures*, 17, 1-27.

Wang, Z., Zhou, S., Zhang, J., Wu, X. and Zhou, L. (2012). "Progressive failure analysis of bolted single-lap composite joint based on extended Finite Element method", *Materials and Design*, 37, 582-588.

Xie, Y., Cao, P. and Liu, L. (2016). "Influence of crack surface friction on crack initiation and propagation: A numerical investigation based on extended Finite Element method", *Computers and Geotechnics*, 74, 1-14.